Conversion of a Catalytic into a Structural Disulfide Bond by Circular Permutation[†]

Jens Hennecke and Rudi Glockshuber*

Institute of Molecular Biology and Biophysics, Eidgenössische Technische Hochschule Hönggerberg, CH-8093 Zürich, Switzerland

Received August 6, 1998; Revised Manuscript Received October 5, 1998

ABSTRACT: The thiol−disulfide oxidoreductase DsbA from *Escherichia coli* is the strongest oxidant of the enzyme family and required for disulfide bond formation in the bacterial periplasm. The catalytic domain of this 189-residue protein has a thioredoxin-like fold and contains a catalytic disulfide bridge that is located within the sequence Cys30-Pro31-His32-Cys33 at the N-terminus of an α-helix. The Cys30−Cys33 disulfide bond destabilizes DsbA by about 16 kJ/mol at pH 7.0, which appears to be caused by the extremely low pK_a value of ∼3.4 of the nucleophilic Cys30 thiol. Here we report the characterization of a circularly permuted variant of DsbA, termed H32−P31, in which the natural termini are connected by a Gly_3-Thr-Gly linker and the new termini are located between the active-site cysteines (first residue His32, last residue Pro31). The disulfide bond in the variant thus connects the second with the penultimate residue. H32−P31 adopts a wild-type-like structure and folds reversibly and cooperatively in both redox forms. However, the permuted variant is catalytically inactive as dithiol oxidase *in vivo* and *in vitro*. Both cysteine thiols have pK_a values > 8; the variant is 500-fold more reducing than the wild type and more stable in its oxidized form. Thus, the Cys30−Cys33 disulfide in the variant H32−P31 has adopted properties of a structural disulfide bond.

Circular permutations in proteins, i.e., linkage of the natural termini and cleavage of the polypeptide at another position, cause changes in the order of the amino acid sequence, secondary structure elements, and possibly domains and thus dramatically alter the polypeptide chain. Rationally designed circular permutants with termini in loop regions have been reported for about 20 different proteins (see, for example, refs *1*−*5* and references cited therein) and have been generated either on the level of the protein, by covalent linkage of the termini and proteolytic cleavage at another position, or by genetic engineering. Strikingly, nearly all these permuted proteins folded properly and showed biological activity. A more rigorous study on the catalytic subunit of aspartate transcarbamoylase by random circular permutation and screening for active proteins showed that even variants with new termini in α-helices are capable of adopting a functional three-dimensional structure (*2*). A prerequisite for circular permutations is the close proximity of the natural N- and C-termini. Even though this is fulfilled in many natural proteins (*6*) and artificial circularly permuted proteins are generally able to fold, the location of termini is usually conserved in proteins, and natural circular permutations, which could arise, for example, by gene duplication and excision, occur only rarely (reviewed in refs *3* and *7*). We recently performed a systematic random circular permutation experiment on the thiol/disulfide oxidoreductase DsbA from the periplasm of *Escherichia coli* (Hennecke and Glockshuber, manuscript submitted for publication) where we created a set of permuted variants so that every loop segment and every regular secondary structure present in the wild-type protein was disrupted. DsbA tolerates new termini in almost every loop region and, strikingly, in most regular secondary structure elements except for four α-helices, which appear to be indispensable for folding and stability of DsbA *in vivo* and *in vitro*. Here, we have constructed a circularly permuted DsbA variant with an even more dramatic alteration by introducing the new termini directly into the α-helix 1 that contains the active site of the protein.

DsbA is a monomeric, 189-residue protein, the main catalyst of disulfide bond formation in the periplasm of *Escherichia coli* (*8*, *9*) and rapidly and randomly introduces disulfide bonds into folding proteins (*10*, *11*). The determination of the three-dimensional structure of oxidized (*12*, *13*) and reduced DsbA (*14*, *15*) has revealed that the enzyme possesses a catalytic, thioredoxin-like domain, which is common to all known structures of disulfide oxidoreductases, and contains a second, α-helical domain of unknown function that is inserted into the thioredoxin motif. The active site of DsbA is formed by a very reactive disulfide bond located within the sequence Cys30-Pro31-His32-Cys33 at the N-terminus of α-helix 1 in the thioredoxin-like domain. DsbA is the strongest oxidant in the family of disulfide oxidoreductases ($E_0' = -0.124 \pm 2$ mV) (*16*−*18*). The oxidative force of the enzyme is mainly caused by the extremely low pK_a of the nucleophilic thiol of Cys30, which has a value of about 3.4 (*19*−*21*). The lowered pK_a explains a very particular feature of DsbA, namely that the Cys30−Cys33 disulfide bond strongly destabilizes the enzyme by about 10−20 kJ/mol (*16*, *22*). *In vivo*, the second step of the catalytic cycle of DsbA, i.e., recycling of the oxidized form of DsbA after disulfide bond transfer to folding polypeptides in the *E. coli*

[†] This project was supported by a research grant from the ETH Zürich.

* To whom correspondence should be addressed. Phone +41-1-633-6819. Fax +41-1-633-1036. E-mail RUDI@MOL.BIOL.ETHZ.CH.

10.1021/bi981888v CCC: $15.00
Published on Web 11/19/1998

periplasm, occurs by a specific disulfide exchange reaction with DsbB, a protein located in the inner membrane of *E. coli* (*23*−*26*).

In the circularly permuted variant of DsbA characterized in this study, termed H32−P31, the natural termini are connected by the pentapeptide linker Gly_3-Thr-Gly and the peptide bond between Pro31 and His32 is broken. Hence, the Cys30−Cys33 disulfide bond in the oxidized variant H32−P31 connects the second and penultimate residue of the protein and introduces a loop formed by the entire polypeptide chain except Pro31 and His32 (amino acid numbering according to wild-type DsbA). We purified the circularly permuted variant H32−P31 from the periplasm of *E. coli* and investigated its ability to adopt a native-like structure in both redox forms and the effect of the Cys30−Cys33 disulfide bond on its thermodynamic stability. In addition, the catalytic activity and biophysical properties of the disulfide bond in H32−P31 were characterized and compared to those of the wild-type protein.

MATERIALS AND METHODS

Materials. DTT,[1] GSH, GSSG, ampicillin, DTNB, X-Gal, and polymyxin B sulfate were purchased from Sigma (Deisenhofen, Germany), Dowex Monosphere mixed-bed ion exchanger, acrylamide, ANS, and bovine pancreatic insulin were from Fluka (Buchs, Switzerland), urea was from U.S. Biochemical Corp. (Cleveland, OH) and maltose and guanidine hydrochloride (GdmCl) were obtained from ICN (Costa Mesa, CA). IPTG was from AGS GmbH (Heidelberg, Germany), DE52- and CM52-cellulose were purchased from Whatman (Maidstone, U.K.), and the phenyl-Superose HR 10/10 column was obtained from Pharmacia (Uppsala, Sweden). All other chemicals were from Merck (Darmstadt, Germany) and of the highest purity available. DNA-modifying enzymes were from AGS GmbH (Heidelberg, Germany), MBI Fermentas (Vilnius, Lithuania), Boehringer Mannheim (Mannheim, Germany), or New England Biolabs (Beverly, MA) except for the Thermo Sequenase sequencing kit, which was obtained from Amersham Pharmacia Biotech (Zürich, Switzerland). Oligonucleotides were purchased from MWG Biotech (Ebersberg, Germany).

Plasmid Construction. The *lac* promoter expression plasmid pDsbA-H32−P31 was constructed from pRBI-PDI (*27*). The gene coding for the circularly permuted variant H32−P31 was obtained by SOE PCR (*28*, *29*), and codons for the Gly_3-Thr-Gly linker were appended to the ends of the mature *dsbA* gene. With the *dsbA* gene in the plasmid pRBI-PDI as template and the 5′-oligonucleotide (PERM3) 5′-AAA GGT GGC GGT ACC GGT GCG CAG TAT GAA GAT GGT AAA C-3′ and the 3′-oligonucleotide (PERM4) 5′-G CCG GAA TTC GGA TCC TTA CGG GCA GAA GAA AGA GAA AAA C-3′ (*Bam*HI site underlined), the 5′ part of the *dsbA* gene coding for A1−P31 was amplified by PCR and purified. The 3′ part coding for H32−K189 was amplified by using the 5′-oligonucleotide (PERM1) 5′-GC CGG AAT TCT AGA GCT CAC TGC TAT CAG TTT GAA A-3′ (*Ecl*136II) and the 3′-oligonucleotide (PERM2) 5′-CTG CGC ACC GGT ACC GCC ACC TTT TTT CTC GGA CAG ATA TTT C-3′ and purified. Both fragments were combined during a subsequent PCR, and the circularly permuted gene was amplified by using the oligonucleotides PERM1 and PERM4. After cleavage with *Ecl*136II and *Bam*HI the fragment was cloned behind the OmpA signal sequence of pRBI-PDI via *Stu*I and *Bam*HI. The circularly permuted gene in the resulting plasmid pOmpA-DsbA(H32−P31) was verified by dideoxynucleotide sequencing.

Determination of DsbA Activity in Vivo. The variant H32−P31 was tested for its ability to complement the phenotypes of *E. coli dsbA*$^-$strains, namely, the lack of motility (*30*) and the ability to inactivate β-galactosidase in the periplasm by oxidation (*9*) as described previously (*18*).

Expression and Purification of cpDsbA. For expression of the variant H32−P31 in the bacterial periplasm, the *E. coli* strain THZ2 (*19*) was used. Cells harboring the plasmid pOmpA-DsbA(H32−P31) were grown at 37 °C in 10 L of 2×YT medium containing 100 μg/mL ampicillin. After induction with 1 mM IPTG at an optical density at 546 nm (OD_{546}) of 1.0, the cells were further grown for 8 h at 37 °C. Periplasmic extracts were first subjected to anion-exchange chromatography (DE52) as described (*18*). Fractions containing DsbA were pooled, adjusted to 1 M ammonium sulfate and pH 8.0 by addition of 4 M ammonium sulfate and 1 M Tris, respectively, and applied to a phenyl-Superose HR10/10 column. The protein was eluted by a linear gradient (100 mL) from 1 to 0 M ammonium sulfate in 20 mM Tris-HCl, pH 8.0. The eluate was concentrated and further subjected to size-exclusion chromatography on Superdex 75 HiLoad 26/60 (Pharmacia) in 50 mM sodium phosphate and 150 mM sodium chloride, pH 7.0. Fractions containing pure H32−P31 were combined, dialyzed against distilled water, and stored at −80 °C. DsbA wild type was purified form the periplasm of *E. coli* THZ2 harboring the plasmid pDSBA2 (*31*).

Protein concentrations were measured by the specific absorbance at 280 nm (*32*) (native, oxidized wild type, ϵ_{280} = 23 300 M^{-1} cm^{-1}; native, oxidized H32−P31, ϵ_{280} = 23 400 M^{-1} cm^{-1}). Both proteins were obtained in the oxidized form after purification, as shown by the lack of free thiol groups (*33*). The molecular mass of the variant H32−P31 was confirmed by ESI mass spectrometry and the correct N-terminus was confirmed by Edman sequencing.

Spectroscopic Measurements. Fluorescence and CD spectra were recorded as described (*34*). Quenching of tryptophan fluorescence by acrylamide was measured in 100 mM sodium phosphate and 1 mM EDTA, pH 7.0, at an emission wavelength of 326 nm (*34*). Binding of ANS to DsbA was analyzed at a protein concentration of 5 μM in 100 mM sodium phosphate and 1 mM EDTA, pH 7.0, by stepwise addition of small aliquots of 10 mM ANS in 50% ethanol. Samples of reduced DsbA additionally contained 5 mM DTT. An excitation wavelength of 360 nm and an emission wavelength of 490 nm was used for the ANS fluorescence measurements.

[1] Abbreviations: ANS, 8-anilinonaphthalene-1-sulfonic acid; CD, circular dichroism; DTNB, 5,5′-dithiobis(2-nitrobenzoic acid); DTT, 1,4-dithio-DL-threitol; GdmCl, guanidinium chloride; GSH, reduced glutathione; EDTA, ethylenediaminetetraacetic acid; ESI, electrospray ionization; GSSG, oxidized glutathione; HPLC, high-performance liquid chromatography; IAM, iodoacetamide; IPTG, isopropyl β-D-thiogalactoside; NADPH, nicotinamide adenine dinucleotide phosphate, reduced; MOPS, 3-(*N*-morpholino)propanesulfonic acid; PCR, polymerase chain reaction; SDS, sodium dodecyl sulfate; SOE, splicing by overlap extension; Tris, 2-amino-2-(hydroxymethyl)-1,3-propanediol; UV, ultraviolet; X-Gal, 5-bromo-4-chloro-3-β-D-galactopyranoside.

Urea-Induced Unfolding Equilibria. For equilibrium unfolding experiments, the native proteins were diluted with degassed 100 mM sodium phosphate, pH 7.0, and 1 mM EDTA containing different concentrations of ultrapure deionized urea and incubated at 25 °C for 2 days. In the case of reduced proteins, 10 mM DTT was included. For refolding experiments, DsbA was denatured by 9.5 M urea or 4 M guanidinium chloride in 100 mM sodium phosphate, pH 7.0, and 1 mM EDTA for 1 h at room temperature and diluted with the above buffer containing different urea concentrations. Transitions were followed by fluorescence ($\lambda_{ex} = 280$ nm; $\lambda_{em} = 322$ nm for the oxidized and reduced variant H32−P31 and oxidized DsbA wild type; $\lambda_{em} = 365$ nm for reduced DsbA wild type) and CD measurements ($\lambda = 219$ nm). Protein concentrations were 1 μM for fluorescence measurements and 12 μM for CD measurements. The EDTA concentration was reduced to 100 μM for all CD measurements. Transitions were evaluated according to a two-state equilibrium with a six-parameter fit as described (*35*).

Determination of the Redox Potential. The redox potentials of DsbA wild type and the variant H32−P31 were determined by measuring the equilibrium constant with glutathione (*17*). DsbA (8 μM) was incubated under a nitrogen atmosphere in 100 mM sodium phosphate, pH 7.0, and 1 mM EDTA for 20 h at 25 °C with different concentrations of GSH (0.01−40 mM) and GSSG (10 or 100 μM). The GSSG concentration present in the reaction mixtures after equilibrium was quantified enzymatically by using NADPH and yeast glutathione reductase (EC 1.6.4.2; Boehringer) in order to account for air oxidation of reduced glutathione during the incubation period and the GSSG contaminations in the GSH stock solution. The assay was performed as described (*36*).

To determine the fraction of reduced DsbA, samples were quenched by addition of formic acid to a final concentration of 10% (v/v) and the reaction products were separated by reversed-phase HPLC on a Vydac 218TP54 C18 column (4.6 × 250 mm) at 55 °C using an acetonitrile gradient [39.0−39.8% (v/v) for DsbA wild type, 25 mL; 38.6−41.8% (v/v) for the variant H32−P31, 14 mL] in 0.1% (v/v) trifluoroacetic acid. The eluted proteins were detected by their absorbance at 280 nm and the fraction of reduced molecules was determined by integration of all peak areas in the elution profiles. The equilibrium constant (K_{eq}) was determined by fitting the original data according to the equation $R = ([GSH]^2/[GSSG])/\{K_{eq}+([GSH]^2/[GSSG])\}$, where R is the fraction of reduced molecules. The redox potential was calculated with the equation $E_0'_{DsbA} = E_0'_{GSH/GSSG} - (RT/2F) \ln (K_{eq})$, with a value of −240 mV for the standard redox potential of glutathione (*37*).

Determination of pK_a Values. To determine the pK_a value of the Cys30 thiol, the pH dependence of its reactivity with iodoacetamide (IAM) was measured (*21*, *38*). The reactions were analyzed by HPLC as described (*39*) except that the eluted proteins were detected at 215 nm. Buffer conditions were the same as described previously (*39*).

Reduction of DsbA by DTT. Since the circularly permuted variant H32−P31 does not show a fluorescence difference between the oxidized and reduced form, the kinetics of reduction could not be measured fluorometrically (*11*, *18*) and were instead followed by analytical HPLC. The oxidized variant H32−P31 (1 μM) was mixed with DTT (5 mM) in 100 mM sodium phosphate and 1 mM EDTA, pH 7.0, or 20 mM potassium phosphate, 20 mM boric acid, 20 mM sodium succinate, 200 mM KCl, and 1 mM EDTA, pH 7.0. The latter buffer had been used to measure the kinetics of reduction of DsbA wild type by DTT (*18*). The reactions were incubated at 25 °C and aliquots of 450 μL were removed after 15, 30, 45, 60, 75, 90, 105, 120, 140, and 160 s and 3, 4, 5, 7, 10, 15, and 60 min and quenched by addition of formic acid and acetonitrile to a final concentration of 10% (v/v) each. The reaction products were separated by reversed-phase HPLC on a Vydac 218TP54 C18 column at 55 °C with an acetonitrile gradient [38.6−41.8% (v/v), 14 mL] in 0.1% (v/v) trifluoroacetic acid. The eluted proteins were detected by their absorbance at 215 nm and the fraction of reduced molecules was determined by integration of the peak areas of the elution profiles. Kinetics were evaluated according to the applied pseudo-first-order conditions.

Reduction of Insulin Disulfides. The spectrometric assay of insulin disulfide reduction was performed in 100 mM potassium phosphate and 2 mM EDTA, pH 7.0, in the presence of 1 μM thioredoxin and 10 μM DsbA wild type, 10 μM H32−P31, or in the absence of enzyme as described (*40*). The reaction was followed by the increase in optical density at 650 nm caused by the precipitation of the reduced insulin A and B chains.

Refolding of Hirudin. Refolding of reduced hirudin by stoichiometric amounts of oxidized DsbA wild type or the circularly permuted variant was performed at pH 7.0 and 25 °C. Reduced, unfolded hirudin was prepared essentially as described (*11*, *41*). Reduced hirudin (28 μM) was mixed with oxidized DsbA (84 μM) in 100 mM sodium phosphate, pH 7.0, and 1 mM EDTA. Aliquots of 120 μL were removed after 1 and 10 min and 1, 6, and 20 h and quenched by addition of formic acid and acetonitrile to a final concentration of 10% (v/v) each. The reaction products were separated by reversed-phase HPLC on a Vydac 218TP54 C18 column at 55 °C using an acetonitrile gradient [20−24% (v/v), 30 mL] in 0.1% (v/v) trifluoroacetic acid. The eluted hirudin species were detected by their absorbance at 230 nm. Refolding of reduced hirudin in the presence of 1 mM GSH, 1 mM GSSG, and catalytic amounts of DsbA (8.4 μM) was performed under the same buffer conditions. Samples were acid-quenched after 15 s, 2.5 and 10 min, and 1, 3, 6, 12, and 24 h and analyzed by HPLC as described above.

RESULTS

Construction, Phenotypic Characterization, and Purification of the Circularly Permuted DsbA Variant H32−P31. The circularly permuted DsbA variant H32−P31 was constructed by SOE PCR (*28*, *29*), cloned behind the OmpA signal sequence, and expressed with yields comparable to those of the wild-type protein in the periplasm of *E. coli* under control of the *lac* promoter/operator sequence. The *in vivo* activity of the variant H32−P31 was tested in the *dsbA*$^-$ strain *E. coli* THZ2 (*19*). Due to the absence of functional DsbA, THZ2 is immotile (*30*) and periplasmically oriented β-galactosidase is not inactivated by random oxidation (*9*). Secretory expression of the variant H32−P31 was able to restore neither motility nor inactivated β-galactosidase in the periplasm of THZ2.

The variant H32−P31 was purified from periplasmic extracts of THZ2 by anion-exchange chromatography, hy-

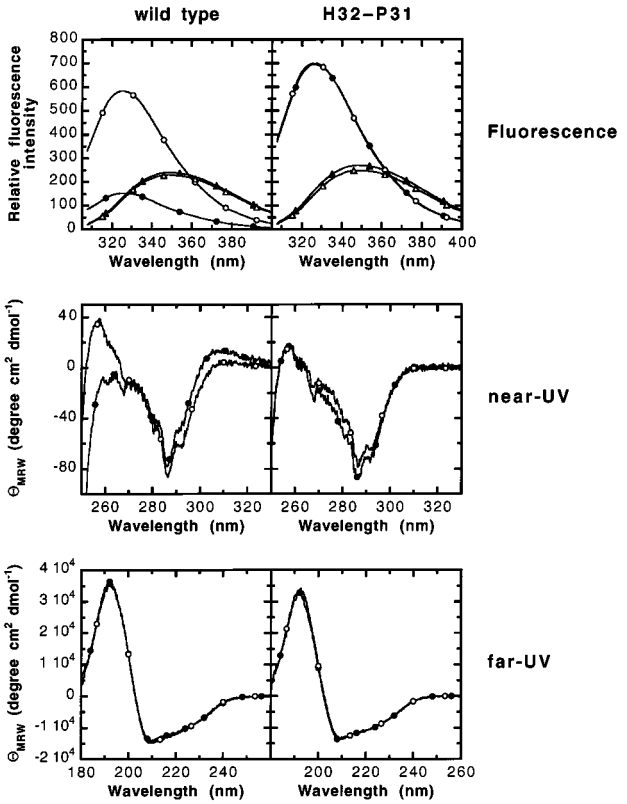

FIGURE 1: Fluorescence spectra (top) and near-UV (middle) and far-UV circular dichroism spectra (bottom) of oxidized and reduced DsbA wild type (left) and the circularly permuted variant H32−P31 (right) at pH 7.0 and 25 °C. Spectra of the native oxidized (●), native reduced (○), unfolded oxidized (▲), and unfolded reduced (△) proteins are shown. For fluorescence spectra, an excitation wavelength of 295 nm was used.

drophobic interaction chromatography, and size-exclusion chromatography with a yield of 25 mg/L of bacterial culture. Edman sequencing and ESI mass spectrometry showed that the OmpA signal sequence was cleaved off correctly and that the protein was not proteolytically degraded. The disulfide bond was completely formed in the purified variant as shown by a band shift compared to a DTT-treated sample on a nonreducing SDS−polyacrylamide gel (data not shown), analytical HPLC (see below), and the lack of free thiol groups (*33*).

Spectroscopic Properties of the Circularly Permuted Variant H32−P31. The overall fold of the variant H32−P31 was compared to that of wild-type DsbA by circular dichroism (CD) spectroscopy (Figure 1). Far-UV CD spectra of H32−P31 are identical to those of the wild-type protein, indicating very similar overall structures. Near-UV CD spectra of DsbA wild type and the variant H32−P31 also show similarities, with a minimum around 286 nm and a maximum at 258 nm and comparable ellipticities. However, the characteristic increase in ellipticity at 258 nm, that is observed upon reduction of the wild-type protein is no longer present in the spectra of H32−P31 (Figure 1).

Analysis of the fluorescence spectra of the H32−P31 variant also revealed redox-state-independent spectroscopic properties, whereas DsbA wild type shows a 4-fold increase in tryptophan fluorescence upon reduction of the active-site disulfide bond. The spectra of the H32−P31 variant showed the same fluorescence maxima as those of oxidized and reduced wild type (324 nm) but an even higher fluorescence

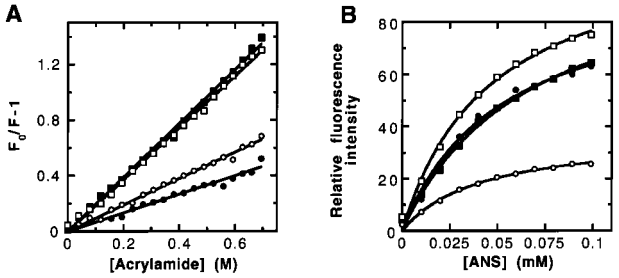

FIGURE 2: Acrylamide-induced quenching of tryptophan fluorescence (A) and binding of ANS (B) at pH 7.0 and 25 °C. Measurements for oxidized (closed symbols) and reduced (open symbols) DsbA wild type (●, ○) and the circularly permuted variant H32−P31 (■, □) are shown. A Stern−Volmer plot is shown (A), where F_0 corresponds to the fluorescence in the absence of acrylamide and F is the measured fluorescence (λ_{ex} = 295 nm; λ_{em} = 326 nm). ANS-binding experiments (B) were performed by stepwise addition of ANS and following the ANS fluorescence change (λ_{ex} = 360 nm; λ_{em} = 490 nm), which was corrected for the volume increase.

than that of reduced DsbA wild type (Figure 1). Obviously, the dynamic fluorescence quenching of the buried Trp76 by the active-site disulfide bond observed for oxidized wild-type DsbA (*34*) is abolished in oxidized H32−P31. Since the Cys30−Cys33 disulfide bond and Trp76 are located in different domains, fluorescence quenching in the oxidized wild type requires a tight interdomain contact. To investigate whether the strongly increased fluorescence of oxidized H32−P31 results from a loosened interdomain contact, we analyzed the solvent accessibility of the tryptophans in the variant and determined the extent of dynamic quenching of their fluorescence by acrylamide. We indeed observed a 2−3-fold stronger acrylamide-induced quenching of the tryptophan fluorescence of H32−P31 as compared to the wild-type protein and, again in contrast to the wild type, redox-state independent quenching (Figure 2A and Table 2). However, we did not obtain any indication of partial unfolding of either redox form of H32−P31. Besides the spectroscopic evidence for a wild-type-like tertiary structure of H32−P31, binding of the hydrophobic dye ANS, which is generally used to identify partially folded states in proteins (*42*), was in the range observed for oxidized and reduced wild-type DsbA (Figure 2B).

Unfolding/Refolding Transitions of DsbA Wild Type and the Circularly Permuted Variant H32−P31. To compare the thermodynamic stabilities of the oxidized and reduced variant H32−P31 with those of oxidized and reduced wild type, we measured urea-induced equilibrium unfolding/refolding transitions at pH 7.0 and 25 °C. The transitions were followed both by the far-UV CD signal at 219 nm, which probes the secondary structure content, and by tryptophan fluorescence, which measures tertiary structure formation (Figure 3, Table 1). All transitions were completely reversible. Despite the almost 2-fold lower cooperativities of the transitions of the permuted variant (Table 1), all transitions were consistent with the two-state model of folding (*35*, *43*) as they were independent of the spectroscopic technique used to follow unfolding within experimental error (Figure 3, Table 1). In contrast to DsbA wild type, where the catalytic disulfide bond destabilized the protein by about 16 kJ/mol under the applied conditions, the oxidized variant H32−P31 was 2−3 kJ/mol more stable than the reduced protein. Overall, the oxidized and reduced forms

Table 1: Thermodynamic Stabilities of Oxidized and Reduced DsbA Wild Type and the Circularly Permuted Variant H32−P31 at 25 °C and pH 7.0[a]

	wild type	H32−P31
Fluorescence		
oxidized		
transition midpoint (M urea)	4.59	4.18
cooperativity (kJ mol^{-1} M^{-1})	10.6 ± 0.3	5.9 ± 0.2
$\Delta\Delta G_{Stab}$ (kJ mol^{-1})	−48.7 ± 1.5	−24.5 ± 0.7
reduced		
transition midpoint (M urea)	5.98	3.20
cooperativity (kJ mol^{-1} M^{-1})	11.0 ± 0.4	7.1 ± 0.2
$\Delta\Delta G_{Stab}$ (kJ mol^{-1})	−66.0 ± 2.4	−22.7 ± 0.7
$\Delta\Delta G_{ox/red}$[b] (kJ mol^{-1})	17.3 ± 3.9	−1.8 ± 1.4
Circular Dichroism		
oxidized		
transition midpoint (M urea)	4.63	4.10
cooperativity (kJ mol^{-1} M^{-1})	10.9 ± 0.5	5.4 ± 0.2
$\Delta\Delta G_{Stab}$ (kJ mol^{-1})	−50.6 ± 2.3	−22.0 ± 0.8
reduced		
transition midpoint (M urea)	6.06	3.20
cooperativity (kJ mol^{-1} M^{-1})	10.7 ± 0.4	5.8 ± 0.8
$\Delta\Delta G_{Stab}$ (kJ mol^{-1})	−64.9 ± 2.2	−18.5 ± 1.0
$\Delta\Delta G_{ox/red}$ (kJ mol^{-1})	14.3 ± 4.5	−3.5 ± 1.8

[a] Urea-induced unfolding/refolding transitions were followed by tryptophan fluorescence and far-UV circular dichroism. Data were evaluated according to the two-state model of folding. [b] $\Delta\Delta G_{ox/red}$ is the difference between the free energies of folding of oxidized and reduced DsbA. A possible influence of the disulfide bond on the entropy of unfolded oxidized DsbA was not considered here.

Table 2: Biochemical and Biophysical Properties of DsbA Wild Type and the Circularly Permuted Variant H32−P31 at 25 °C and pH 7.0

	wild type	H32−P31
activity *in vivo*	+	−
hirudin refolding: $t_{1/2}$[a]	4 ± 0.5 min	≥ 7 days
K_{eq} with glutathione (mM)	0.126 ± 0.005	68.2 ± 1.2
E_0' (mV)[b]	−125	−206
pK_a of the Cys30 thiol	3.4[c]	≥8
reduction by DTT: $k_{2ndorder}$ (M^{-1} s^{-1})	55 500 ± 2000	2.40 ± 0.31
K_D[d] (M^{-1} acrylamide)		
oxidized	0.66 ± 0.02	1.94 ± 0.03
reduced	0.95 ± 0.02	1.86 ± 0.03

[a] $t_{1/2}$ is the half time of refolding of reduced hirudin with stoichiometric amounts of oxidized DsbA. [b] The redox potential of DsbA was calculated from the equilibrium constant with GSH/GSSG using an E'_0 of −240 mV for GSH/GSSG. [c] The ionization of the Cys30 side chain was detected by the specific absorbance of the thiolate anion at 240 nm. [d] K_D is the Stern−Volmer quenching constant: $F/F_0 = 1 + K_D$[acrylamide], where F_0 corresponds to the fluorescence in the absence of acrylamide and F is the measured fluorescence.

of the variant were both significantly less stable than oxidized DsbA wild type, which is reflected by transition midpoints at lower urea concentrations and lower cooperativities of folding (Figure 3, Table 1).

Redox Properties of the Circularly Permuted Variant H32−P31. As the dipeptide Pro31-His32 between the active-site cysteines has been shown to be an important factor for the oxidative force of DsbA (*19*, *20*) and the new termini in the permuted variant disrupt the Pro31−His32 peptide bond, we investigated the redox potential of the variant by measuring its equilibrium constants (K_{eq}) with glutathione at pH 7.0 and 25 °C. As the redox state of the variant at different GSH/GSSG ratios cannot be detected fluorometrically as in the case of the wild type (Figure 1; *17*), the equilibria were frozen by the addition of acid and the

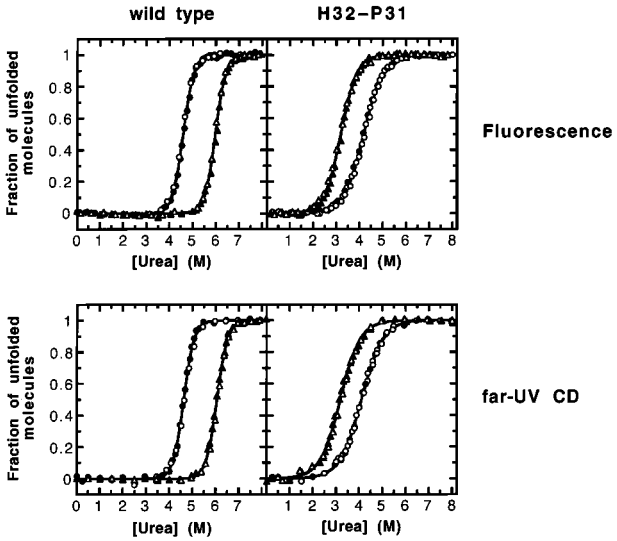

FIGURE 3: Urea-induced unfolding/refolding equilibrium transitions of oxidized (●, ○) and reduced (▲, △) DsbA wild type (left) and the circularly permuted variant H32−P31 (right) at pH 7.0 and 25 °C. Unfolding and refolding experiments are represented by closed and open symbols, respectively. The transitions were followed by fluorescence (λ_{ex} = 280 nm; λ_{em} = 322 nm for oxidized and reduced H32−P31 and oxidized wild type and 365 nm for reduced wild type) or far-UV CD measurements (λ = 219 nm) and normalized. The solid lines represent a six-parameter fit according to the two-state model of folding (*35*).

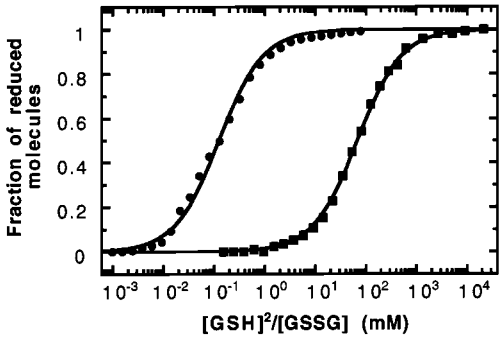

FIGURE 4: Redox equilibria of DsbA wild type (●) and the circularly permuted variant H32−P31 (■) with glutathione at pH 7.0 and 25 °C. Proteins were incubated with different ratios of reduced to oxidized glutathione and the fraction of reduced DsbA in each sample was determined by analytical HPLC after acid quenching of disulfide exchange. The solid lines represent fits according to the DsbA/glutathione equilibrium (see Materials and Methods).

oxidized and reduced forms of the proteins were separated by analytical reversed-phase HPLC and quantified (Figure 4). With a redox potential of −206 mV, the permuted variant H32−P31 is indeed 81 mV more reducing than DsbA wild type (E_0' = −125 mV), corresponding to a 540-fold higher equilibrium constant with glutathione (Figure 4, Table 2). However, the lowered redox potential of H32−P31 alone is not sufficient to explain its lack of activity in the variant H32−P31 *in vivo*, since other variants of DsbA with even lower redox potentials (up to −214 mV) have been shown to complement *dsbA* deficiency *in vivo* (*19*, *20*).

Catalytic Properties of the Circularly Permuted DsbA Variant H32−P31. To test whether the variant H32−P31 is inactive *in vivo* because it is not efficiently recycled as oxidant by DsbB or because it is not capable of efficiently oxidizing folding proteins in the periplasm, we probed its

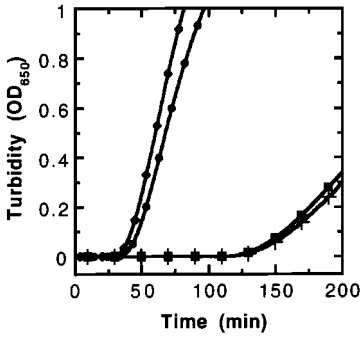

FIGURE 5: Reduction of insulin disulfides by DTT in the presence of catalytic amounts of DsbA wild type and the circularly permuted variant H32−P31 at pH 7.0 and 25 °C. Reduction of insulin (131 μM) was initiated by the addition of 0.33 mM DTT in the presence of either 10 μM DsbA wild type (●), 10 μM H32−P31 (■), or 1 μM *E. coli* thioredoxin (◆) or in the absence of enzyme (+). Aggregation of reduced insulin was followed by the increase in optical density at 650 nm.

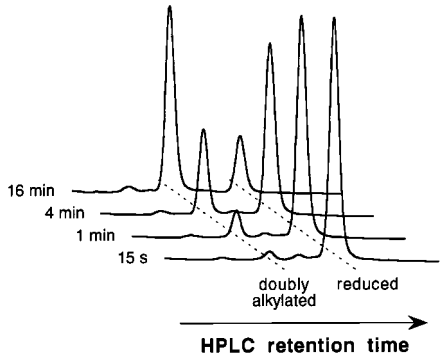

FIGURE 6: HPLC analysis of the reaction of the native, reduced circularly permuted variant H32−P31 with iodoacetamide (IAM) at pH 8.0 and 25 °C. The reaction was performed under pseudo-first-order conditions (1 μM H32−P31, 0.4 mM IAM) and quenched after different times with formic acid/acetonitrile. The reaction products were separated on an analytical C18 reversed-phase HPLC column and detected by their absorbance at 215 nm. The monoalkylated forms of H32−P31 did not accumulate as intermediates in significant amounts during the reaction.

ability to act as thiol oxidase and disulfide isomerase on folding proteins *in vitro* using hirudin as a polypeptide substrate. After complete reduction of its three intramolecular disulfide bonds (*41*, *44*, *45*), unfolded hirudin was stoichiometrically oxidized with 3 molar equivalents of oxidized DsbA wild type and the oxidized variant H32−P31 at pH 7.0. Formation of oxidized folding intermediates and recovery of native hirudin was analyzed by HPLC separation of the acid-quenching folding reactions after different times of refolding. DsbA wild type very efficiently oxidizes hirudin in a random fashion so that fully reduced hirudin can no longer be detected after 15 s. Reduced DsbA wild type then isomerizes the nonnative disulfide bonds in a slower process (*11*) so that native hirudin is formed with a half-time of 4 min at pH 7.0 and 25 °C (data not shown; Table 2). In contrast, oxidation of hirudin by the variant H32−P31 was at least 10 000-fold slower so that completely reduced hirudin was still present after 30 min of refolding. Native hirudin was formed with a half-time of about 7 days. Compared to the stoichiometric oxidation of hirudin with oxidized glutathione, oxidative refolding with the variant H32−P31 is only 2−4 times faster. We conclude that the lack of disulfide oxidase activity of the variant H32−P31 is responsible for its inability to complement DsbA deficiency.

We also measured the ability of H32−P31 to catalyze a reverse reaction, i.e., the reduction of insulin disulfides by DTT (*40*). The three disulfide bridges of insulin were reduced by DTT at pH 7.0 in the absence and presence of catalytic amounts of DsbA wild type and H32−P31, and the reaction was followed by the increase of the optical density at 650 nm caused by aggregation of reduced insulin chains. In contrast to wild-type DsbA, the variant H32−P31 practically lacked insulin reductase activity (Figure 5). To test whether this results from slow recycling of the reduced variant by DTT, H32−P31 was reduced by DTT at pH 7.0 under pseudo-first-order conditions (5000-fold molar excess of DTT) and the reaction was followed by analytical HPLC. The reaction indeed turned out to be extremely slow with a deduced second-order rate constant of 2.4 M^{-1} s^{-1} (Table 2). The disulfide bond in the variant H32−P31 is thus approximately 10^4 times less reactive than that of wild-type DsbA (Table 2) (*18*), providing a plausible explanation for the extremely low insulin reductase activity of H32−P31.

Thiol−disulfide interchange reactions are strongly dependent on the pK_a values of the involved thiols (*46*). Accordingly, the extremely low pK_a of Cys30 in wild-type DsbA can almost quantitatively explain the extremely fast disulfide exchange reactions of the enzyme (*21*). To investigate whether the low reactivity of the permuted variant H32−P31 is caused by increased pK_a values of the Cys30 and/or Cys33 thiols, the pH dependence of the reaction of reduced H32−P31 with IAM was analyzed (*38*) in the range of pH 5.0−10.5. The reactions were acid-quenched after different times and analyzed by reversed-phase HPLC. The monoalkylated forms of H32−P31 did not accumulate in significant amounts and only a single reaction product was observed with a molecular mass exactly corresponding to the doubly alkylated protein (Figure 6). This observation is in contrast to the reduced wild-type protein, in which only the solvent-accessible Cys30 thiol reacts with IAM in the native state (*39*, *47*). Since no monoalkylated protein species were detectable, we could not evaluate the individual rate constants for the alkylation of Cys30 and Cys33 and thus could also not determine the individual pK_a values (data not shown). Nevertheless, the formation of the doubly alkylated protein was strongly dependent on pH. The reaction was below the detection limit at pH values <7.0 and still became faster above pH 10.5. We can thus estimate that both cysteine thiols have a pK_a of at least 8, so that the pK_a of the Cys30 thiol must be increased by more than 4 units compared to that of the wild-type protein (Table 2).

DISCUSSION

The permuted DsbA variant H32−P31 represents an extreme case of a circular permutation in that its new termini disrupt not only a regular secondary structure, i.e., helix α1, but also the active-site sequence Cys30-Pro31-His32-Cys33, which has been shown to be extremely important for stability and function of DsbA (*19*, *20*). Another particular feature of the H32−P31 variant is that formation of the Cys30−Cys33 disulfide bond transforms the linear polypeptide chain into a covalently closed, circular polypeptide as it connects the second with the penultimate residue. Despite the dramatic changes introduced into the polypeptide chain of

H32−P31, the protein is capable of adopting a tertiary structure that is very similar to that of DsbA wild type and to fold cooperatively and reversibly in both redox forms. An obvious spectroscopic difference between wild-type DsbA and H32−P31 is that redox-state-specific, local structural differences that are observable for the wild-type with near-UV CD and fluorescence spectra, acrylamide-induced fluorescence quenching, and ANS binding are no longer detected in the variant. This is in accordance with the almost identical thermodynamic stabilities of the oxidized and reduced form of H32−P31.

The Cys30−Cys33 disulfide bridge in DsbA wild type exhibits ideal properties for catalyzing disulfide bond formation in reduced polypeptide substrates. It is the most oxidizing protein disulfide identified so far (*16*, *17*), strongly destabilizing DsbA and oxidizes organic thiols and reduced polypeptide substrates with second-order rate constants close to the diffusion limit (*10*, *11*, *18*, *48*). These properties are mainly conferred by the extremely low pK_a of the Cys30 thiol (*19*−*21*), which is assumed to result from an interaction of the Cys30 thiolate with the dipole of the active-site α-helix (*14*, *49*−*51*), electrostatic interaction with the His32 side chain (*13*, *51*, *52*), and formation of hydrogen bonds with either Cys33Sγ, His32NH, His32Nδ1, or Cys33NH (*15*). In contrast, the Cys30−Cys33 disulfide bond in the circularly permuted variant H32−P31 lacks all features of a catalytic disulfide bond, and the variant is inactive both *in vivo* and *in vitro*. Specifically, the pK_a of the Cys30 thiol is increased to a value of >8, and the pK_a of Cys33 in H32−P31 also has a similar value. The pK_a values of both cysteines are thus close to the pK_a of 9.5 of a "normal" cysteine residue. As expected from the theory on the rate constants of disulfide exchange reactions (*21*, *46*) the H32−P31 variant is significantly less oxidizing than the wild type. The 540-fold increased equilibrium constant with glutathione of 68.2 mM has thus also come close to the known values of stabilizing, structural disulfide bonds, which are in the range between 1 and 10^7 M (*53*). The rate constants of the reaction between oxidized DsbA and organic thiols or reduced polypeptide substrates suffered an even larger change with an at least 10^4-fold lower reactivity of the variant H32−P31. The measured rate constant for the reduction of H32−P32 with DTT at pH 7.0 of 2.4 M^{-1} s^{-1} is indeed in the range observed for structural disulfide bonds (*54*). Another remarkable feature of the reduced H32−P31 variant is the solvent accessibility of the Cys33 thiol, which exhibits a very similar reactivity as the thiol of Cys30 (Figure 6). In contrast, Cys33 is completely buried in the reduced wild type and does not react with IAM (*21*). This suggests that the structure of reduced H32−P31 is loosened in the vicinity of Cys33 and that its C-terminus with Cys30-Pro31 as the last residues may even be rather flexible. Overall, the disulfide bond in the variant H32−P31 has adopted many features of a structural disulfide bond.

The urea-induced unfolding/refolding transitions of the oxidized and reduced variant H32−P31 demonstrate that the variant is significantly destabilized compared to the wild-type protein. Obviously, the linkage of the original termini and/or the location of the new termini in the beginning of the active-site α-helix 1 is energetically unfavorable. In contrast to DsbA wild type, the oxidized form of the variant H32−P31 is more stable than the reduced form, which is the prerequisite for a structural disulfide bond. Since the disulfide bond of the variant H32−P31 covalently links the second residue of the polypeptide chain with the penultimate residue, an almost circular polypeptide results in oxidized H32−P31, which is expected to have a much lower conformational entropy in the denatured state compared to denatured, reduced H32−P31. This entropy difference can principally be calculated from

$$\Delta S = -8.8\ \mathrm{J\ K^{-1}\ mol^{-1}} - (3/2)R \ln n$$

in which R is the gas constant and n is the number of residues (4 for DsbA wild type, 192 for H32−P31) in the polypeptide loop forming the disulfide bond (*55*). If only the entropy loss in the unfolded, oxidized state of H32−P31 determined the stability difference between the oxidized and reduced variant, the oxidized protein should be 22.2 kJ/mol more stable than the reduced variant. As oxidized H32−P31 is only 1.8−3.5 kJ/mol more stable than the reduced protein, the gain in folding stability of oxidized H32−P31 caused by the reduced entropy of the unfolded protein appears to be almost completely compensated by other factors such as steric strain, unfavorable interactions of the new termini with charged residues that may be more remote in the reduced form, or a loss of chain entropy in native, oxidized H32−P31 if the C-terminal segment is flexible in the reduced variant (see above). All these destabilizing factors thus comprise about 20 kJ/mol for the reduced H32−P31 variant.

For the entropic reasons given above (*55*), the introduction of new cross-links, especially newly designed disulfide bonds, at new positions into polypeptides has been considered as a useful tool for the stabilization of proteins by rational means (*56*−*60*). However, engineered disulfide bonds were sometimes even destabilizing as unpredicted factors such as steric strains occurred or the disulfide bond adopted unfavorable dihedral angles (*61*−*63*). An observation analogous to the stability difference between oxidized and reduced H32−P31 was also made with completely circularized bovine pancreatic trypsin inhibitor (BPTI), where linkage of the termini by a peptide bond had only minor effects on the stability and the folding of the protein (*1*, *64*). Conversely, however, linkage of the termini of chymotrypsin inhibitor 2 by a disulfide bond stabilized the protein and accelerated folding 7-fold, presumably by narrowing the conformational space (*5*). Rational circular permutation of disulfide-bonded proteins principally allows the modulation of the number of residues within the loops formed by the disulfide bonds. Such a strategy may prove to be very useful in the future to generate proteins with increased stability since it makes use of an already existing disulfide bond, the local environment of which is assumed to change little upon circular permutation (*65*). In this context, the H32−P31 variant represents an interesting example as its three-dimensional structure is almost unaffected compared to the wild type.

ACKNOWLEDGMENT

We thank Dr. M. Huber-Wunderlich, Dr. A. Jacobi, Dr. S. Liemann, and P. Sebbel for many fruitful discussions, Dr. P. James for recording the mass spectra, Dr. G. Frank for N-terminal sequencing, and E. Mössner for providing us with *E. coli* thioredoxin.

REFERENCES

1. Goldenberg, D. P., and Creighton, T. E. (1983) *J. Mol. Biol. 165*, 407−413.
2. Graf, R., and Schachman, H. K. (1996) *Proc. Natl. Acad. Sci. U.S.A. 93*, 11591−11596.
3. Heinemann, U., and Hahn, M. (1995) *Prog. Biophys. Mol. Biol. 64*, 121−143.
4. Luger, K., Hommel, U., Herold, M., Hofsteenge, J., and Kirschner, K. (1989) *Science 243*, 206−210.
5. Otzen, D. E., and Fersht, A. R. (1998) *Biochemistry 37*, 8139−8146.
6. Thornton, J. M., and Sibanda, B. L. (1983) *J. Mol. Biol. 167*, 443−460.
7. Lindqvist, Y., and Schneider, G. (1997) *Curr. Opin. Struct. Biol. 7*, 422−427.
8. Kamitani, S., Akiyama, Y., and Ito, K. (1992) *EMBO J. 11*, 57−62.
9. Bardwell, J. C. A., McGovern, K., and Beckwith, J. (1991) *Cell 67*, 581−589.
10. Zapun, A., and Creighton, T. E. (1994) *Biochemistry 33*, 5202−5211.
11. Wunderlich, M., Otto, A., Seckler, R., and Glockshuber, R. (1993) *Biochemistry 32*, 12251−12256.
12. Martin, J. L., Bardwell, J. C. A., and Kuriyan, J. (1993) *Nature 365*, 464−468.
13. Guddat, L. W., Bardwell, J. C. A., Zander, T., and Martin, J. L. (1997) *Protein Sci. 6*, 1148−1156.
14. Schirra, H. J., Renner, C., Czisch, M., Huber-Wunderlich, M., Holak, T. A., and Glockshuber, R. (1998) *Biochemistry 37*, 6263−6276.
15. Guddat, L. W., Bardwell, J. C. A., and Martin, J. L. (1998) *Structure 6*, 757−767.
16. Zapun, A., Bardwell, J. C. A., and Creighton, T. E. (1993) *Biochemistry 32*, 5083−5092.
17. Wunderlich, M., and Glockshuber, R. (1993) *Protein Sci. 2*, 717−726.
18. Hennecke, J., Spleiss, C., and Glockshuber, R. (1997) *J. Biol. Chem. 272*, 189−195.
19. Grauschopf, U., Winther, J. R., Korber, P., Zander, T., Dallinger, P., and Bardwell, J. C. A. (1995) *Cell 83*, 947−955.
20. Huber-Wunderlich, M., and Glockshuber, R. (1998) *Folding Des. 3*, 161−171.
21. Nelson, J. W., and Creighton, T. E. (1994) *Biochemistry 33*, 5974−5983.
22. Wunderlich, M., Jaenicke, R., and Glockshuber, R. (1993a) *J. Mol. Biol. 233*, 559−566.
23. Bardwell, J. C. A., Lee, J.-O., Jander, G., Martin, N., Belin, D., and Beckwith, J. (1993) *Proc. Natl. Acad. Sci. U.S.A. 90*, 1038−1042.
24. Bader, M., Muse, W., Zander, T., and Bardwell, J. (1998) *J. Biol. Chem. 273*, 10302−10307.
25. Guilhot, C., Jander, G., Martin, N. L., and Beckwith, J. (1995) *Proc. Natl. Acad. Sci. U.S.A. 92*, 9895−9899.
26. Kishigami, S., and Ito, K. (1996) *Genes Cells 1*, 201−208.
27. Wunderlich, M., and Glockshuber, R. (1993) *J. Biol. Chem. 268*, 24547−24550.
28. Yon, J., and Fried, M. (1989) *Nucleic Acids Res. 17*, 4895.
29. Horton, R. M., Ho, S. N., Pullen, J. K., Hunt, H. D., Cai, Z., and Pease, L. R. (1993) *Methods Enzymol. 217*, 270−279.
30. Dailey, F. E., and Berg, H. C. (1993) *Proc. Natl. Acad. Sci. U.S.A. 90*, 1043−1047.
31. Jacobi, A., Huber-Wunderlich, M., Hennecke, J., and Glockshuber, R. (1997) *J. Biol. Chem. 272*, 21692−21699.
32. Gill, S. C., and von Hippel, P. H. (1989) *Anal. Biochem. 182*, 319−326.
33. Ellman, G. L. (1959) *Arch. Biochem. Biophys. 82*, 70−77.
34. Hennecke, J., Sillen, A., Huber-Wunderlich, M., Engelborghs, Y., and Glockshuber, R. (1997) *Biochemistry 36*, 6391−6400.
35. Santoro, M. M., and Bolen, D. W. (1988) *Biochemistry 27*, 8063−8068.
36. Loferer, H., Wunderlich, M., Hennecke, H., and Glockshuber, R. (1995) *J. Biol. Chem. 270*, 26178−26183.
37. Rost, J., and Rapoport, S. (1964) *Nature 201*, 185.
38. Kallis, G.-B., and Holmgren, A. (1980) *J. Biol. Chem. 255*, 10261−10265.
39. Mössner, E., Huber-Wunderlich, M., and Glockshuber, R. (1998) *Protein Sci. 7*, 1233−1244.
40. Holmgren, A. (1979) *J. Biol. Chem. 254*, 9627−9632.
41. Otto, A., and Seckler, R. (1991) *Eur. J. Biochem. 202*, 67−73.
42. Eftink, M. R. (1997) *Methods Enzymol. 278*, 221−257.
43. Pace, C. N. (1986) *Methods Enzymol. 131*, 266−280.
44. Szyperski, T., Güntert, P., Stone, S. R., Tulinsky, A., Bode, W., Huber, R., and Wüthrich, K. (1992) *J. Mol. Biol. 228*, 1206−1211.
45. Dodt, J., Seemüller, U., Maschler, R., and Fritz, H. (1985) *Biol. Chem. Hoppe-Seyler 366*, 379−385.
46. Szajewski, R. P., and Whitesides, G. M. (1980) *J. Am. Chem. Soc. 102*, 2011−2026.
47. Zapun, A., Cooper, L., and Creighton, T. E. (1994) *Biochemistry 33*, 1907−1914.
48. Darby, N. J., and Creighton, T. E. (1995) *Biochemistry 34*, 3576−3587.
49. Hol, W. G. J. (1985) *Prog. Biophys. Mol. Biol. 45*, 149−195.
50. Kortemme, T., and Creighton, T. E. (1995) *J. Mol. Biol 253*, 799−812.
51. Kortemme, T., Darby, N. J., and Creighton, T. E. (1996) *Biochemistry 35*, 14503−14511.
52. Warwicker, J., and Gane, P. J. (1996) *FEBS Lett. 385*, 105−108.
53. Gilbert, H. F. (1990) *Adv. Enzymol. Relat. Areas Mol. Biol. 63*, 69−172.
54. Shaked, Z., Szajewski, R. P., and Whitesides, G. M. (1980) *Biochemistry 19*, 4156−4166.
55. Pace, C. N., Grimsley, G. R., Thomson, J. A., and Barnett, B. J. (1988) *J. Biol. Chem. 263*, 11820−11825.
56. Matsumura, M., Becktel, W. J., Levitt, M., and Matthews, B. W. (1989) *Proc. Natl. Acad. Sci. U.S.A. 86*, 6562−6566.
57. Matsumura, M., Signor, G., and Matthews, B. W. (1989) *Nature 342*, 291−293.
58. Pantoliano, M. W., Ladner, R. C., Bryan, P. N., Rollence, M. L., Wood, J. F., and Poulos, T. L. (1987) *Biochemistry 26*, 2077−2082.
59. Lee, B., and Vasmatzis, G. (1997) *Curr. Opin. Biotechnol. 8*, 423−428.
60. Betz, S. F. (1993) *Protein Sci. 2*, 1551−1558.
61. Betz, S. F., and Pielak, G. J. (1992) *Biochemistry 31*, 12337−12344.
62. Betz, S. F., Marmorino, J. L., Saunders, A. J., Doyle, D. F., Young, G. B., and Pielak, G. J. (1996) *Biochemistry 35*, 7422−7428.
63. Hinck, A. P., Truckses, D. M., and Markley, J. L. (1996) *Biochemistry 35*, 10328−10338.
64. Goldenberg, D. P., and Creighton, T. E. (1984) *J. Mol. Biol. 179*, 527−545.
65. Zhang, T., Bertelsen, E., and Alber, T. (1994) *Nat. Struct. Biol. 1*, 434−438.

BI981888V